Expression of p16^{Ink4a} Compensates for *p18^{Ink4c}* Loss in Cyclin-Dependent Kinase 4/6–Dependent Tumors and Tissues

Matthew R. Ramsey,[1,4] Janakiraman Krishnamurthy,[1] Xin-Hai Pei,[2] Chad Torrice,[1] Weili Lin,[3] Daniel R. Carrasco,[5,6] Keith L. Ligon,[6] Yue Xiong,[2] and Norman E. Sharpless[1]

Departments of [1]Medicine and Genetics, [2]Biochemistry and Biophysics, and [3]Neurology and [4]Curriculum in Genetics and Molecular Biology, The Lineberger Comprehensive Cancer Center, The University of North Carolina School of Medicine, Chapel Hill, North Carolina; [5]Department of Adult Oncology, Dana-Farber Cancer Institute, Harvard Medical School; and [6]Department of Pathology, Brigham and Women's Hospital and Harvard Medical School, Boston, Massachusetts

Abstract

Cell cycle progression from G_1 to S phase depends on phosphorylation of pRb by complexes containing a cyclin (D type or E type) and cyclin-dependent kinase (e.g., cdk2, cdk4, or cdk6). Ink4 proteins function to oppose the action of cdk4/6-cyclin D complexes by inhibiting cdk4/6. We employed genetic and pharmacologic approaches to study the interplay among Ink4 proteins and cdk4/6 activity *in vivo*. Mouse embryo fibroblasts (MEF) lacking *p16^{Ink4a}* and *p18^{Ink4c}* showed similar growth kinetics as wild-type MEFs despite increased cdk4 activity. *In vivo*, germline deficiency of *p16^{Ink4a}* and *p18^{Ink4c}* resulted in increased proliferation in the intermediate pituitary and pancreatic islets of adult mice, and survival of *p16$^{Ink4a-/-}$;p18$^{Ink4c-/-}$* mice was significantly reduced due to aggressive pituitary tumors. Compensation among the Ink4 proteins was observed both *in vivo* in *p18$^{Ink4c-/-}$* mice and in MEFs from *p16$^{Ink4a-/-}$*, *p18$^{Ink4c-/-}$*, or *p16$^{Ink4a-/-}$;p18$^{Ink4c-/-}$* mice. Treatment with PD 0332991, a specific cdk4/6 kinase inhibitor, abrogated proliferation in those compartments where Ink4 deficiency was associated with enhanced proliferation (i.e., islets, pituitary, and B lymphocytes) but had no effect on proliferation in other tissues such as the small bowel. These data suggest that *p16^{Ink4a}* and *p18^{Ink4c}* coordinately regulate the *in vivo* catalytic activity of cdk4/6 in specific compartments of adult mice. [Cancer Res 2007;67(10):4732–41]

Introduction

Control of the retinoblastoma family proteins (pRb, p107, and p130) through phosphorylation by cyclin-dependent kinases (cdk) is essential for cell cycle regulation. Cdks require cyclin cofactors for their activity, and cyclin-cdk pairs have been shown to be active at the G_1-S boundary. Cdk2 can bind to cyclin E1, cyclin E2, or cyclin A, whereas cdk4 and cdk6 have been found to pair with the D-type cyclins (reviewed in ref. 1). The activity of these complexes is tightly controlled by both periodic synthesis and destruction of cyclins as well as by cdk inhibitor proteins.

The Ink4 family of cdk inhibitors consists of four members [p16^{Ink4a} (2), p15^{Ink4b} (3), p18^{Ink4c} (4), and p19^{Ink4d} (5)], and all are specific inhibitors of cdk4/6-cyclin D complexes. Both p16^{Ink4a} and p15^{Ink4b} consist of four ankyrin repeats, with ~80% sequence similarity to each other, whereas p18^{Ink4c} and p19^{Ink4d} have a fifth ankryin repeat (reviewed in ref. 6). All four inhibit cdk4 and cdk6 by binding opposite the cyclin binding site, causing an allosteric shift and blocking cyclin binding and ATP hydrolysis (7, 8). Although there have been some reported differences in the regulation of different Ink4s (9–11), they seem to bind cdk4 and cdk6 with comparable affinity (12). In general, distinct roles for these proteins *in vivo* have not been delineated, although p16^{Ink4a} in particular has been associated with senescence and tumor suppression (reviewed in ref. 13).

Despite the biochemical similarities, mice lacking individual *Ink4* genes exhibit different phenotypes. Mice lacking *p19^{Ink4d}* mice are overtly normal but have testicular atrophy and deafness (14, 15). Mice lacking *p15^{Ink4b}* show increased proliferation in the lymphoid lineages and a low incidence of spontaneous tumor formation (16). On the other hand, both *p16$^{Ink4a-/-}$* (17–19) and *p18$^{Ink4c-/-}$* (16, 20) mice exhibit increased susceptibility to spontaneous and carcinogen-induced tumors, but with minimal overlap of tumor spectrum. Mice lacking *p16^{Ink4a}* develop spontaneous lymphomas and sarcomas at low penetrance, whereas the majority of *p18$^{Ink4c-/-}$* mice develop pituitary tumors of the intermediate lobe, suggesting different *in vivo* roles for these proteins.

Elucidation of the control of the proliferative cdks by the partially redundant cdk inhibitors remains a major hurdle in the clear understanding of the cell cycle, a problem made more difficult by the compensation seen among family members. In this study, we have investigated the effects of combined loss of *p16^{Ink4a}* and *p18^{Ink4c}* *in vitro* and *in vivo*. We show that in murine embryo fibroblasts (MEF), the loss of *p18^{Ink4c}* results in compensatory increases in p16^{Ink4a}, whereas loss of *p16^{Ink4a}* is associated with increased expression of p15^{Ink4b}. *In vivo*, the loss of *p18^{Ink4c}* results in compensatory increases in p16^{Ink4a} in various organs, which restrains proliferation. Additionally, using genetic and pharmacologic approaches, we show that specific *in vivo* compartments in the adult mouse are exquisitely dependent on cdk4/6 kinase activity for proliferation. These data suggest that p16^{Ink4a} and p18^{Ink4c} function to regulate physiologic and aberrant proliferation in specific compartments of adult mice.

Materials and Methods

Mouse colony and cell culture. Animals were generated and genotyped as previously described (18, 20) and were N1 in FVB. Mice were housed and treated in accordance with protocols approved by the institutional care and use committee for animal research at the University of North Carolina. Murine *p16^{Ink4a}* and *p18^{Ink4c}* are located 18 cM apart on chromosome 4,

Note: Supplementary data for this article are available at Cancer Research Online (http://cancerres.aacrjournals.org/).

Requests for reprints: Norman E. Sharpless, Departments of Medicine and Genetics, The Lineberger Comprehensive Cancer Center, The University of North Carolina School of Medicine, CB# 7295, Chapel Hill, NC 27599-7295. Phone: 919-966-1185; Fax: 919-966-8212; E-mail: nes@med.unc.edu.

©2007 American Association for Cancer Research.

doi:10.1158/0008-5472.CAN-06-3437

requiring a modified breeding scheme of crossing two double heterozygotes in *cis* or two double heterozygotes in *trans* to generate the colony. For survival analyses, animals were examined thrice per week. Rare deaths of unknown cause (n = 5) were censored from tumor-free analysis, but their inclusion does not change the conclusions. Islet size was quantified using Image-Pro Express software on 115 to 215 individual islets from at least two mice per genotype at 35 weeks of age. To assess proliferation after cdk4/6 inhibition, mice were treated daily for 2 weeks by oral gavage with 150 mg/kg of 87.11 mmol/L PD 0332991 (Pfizer) dissolved in 50 mmol/L sodium lactate buffer (pH 4.0), or buffer alone as described (21).

MEFs were cultured from whole 13.5-day-old embryos as described (18) and grown at 21%O_2, 5% CO_2. Cumulative population doublings were calculated as Log_2 (number of cells at harvest/number of cells plated). Transformations with *H-Ras*^{V12G} and *SV40 TAg* and high-density seeding assays were done as previously described (22) with duplicate samples from four to six lines of each genotype.

Western blotting and immunoprecipitation kinase assays. Western blot assays were done as described (19). Antibodies against $p21^{Cip1}$ (F-8, Santa Cruz), $p16^{Ink4a}$ (M-156, Santa Cruz), actin (C-1, Santa Cruz), cyclin D1 (DCS-6, Cell Signaling), cyclin E (M-20, Santa Cruz), cdk2 (M2, Santa Cruz), and cdk4 (C-22, Santa Cruz) are commercially available. Antibodies to $p15^{Ink4b}$, $p18^{Ink4c}$, and $p27^{Kip1}$ have been previously described (20). Antibody against $p19^{Ink4d}$ was raised against a COOH-terminal peptide, and affinity was purified.

Kinase assays were done on MEFs as described (23), with some modifications. Briefly, fresh cells were lysed for 45 min at 4°C in NP40 buffer [50 mmol/L Tris (pH 7.5), 150 mmol/L NaCl, 0.5% NP40, phosphatase inhibitor cocktail I and II (Calbiochem)]; 100 μg (cdk2) or 900 μg (cdk4) total protein was immunoprecipitated with antibodies specified above. Lysates were precleared twice with 50 μL protein A agarose beads and immunoprecipitated for 12 h at 4°C. Beads were rinsed thrice with cold NP40 buffer, then twice with cold kinase assay buffer [50 mmol/L HEPES (pH 7.0), 10 mmol/L $MgCl_2$, 5 mmol/L $MnCl_2$, 1 mmol/L DTT, 5 μmol/L ATP]. Reactions were done in 30 μL kinase buffer with 5 μCi [γ-^{32}P]ATP (3,000 Ci/mmol) and 1 μL GST-Rb substrate (Santa Cruz, Rb769). Reactions were carried out for 30 min at 30°C. SDS sample buffer was then added; lysates were boiled for 3 min; and protein was separated on 12.5% bis-acrylamide gels.

Immunohistochemistry. Assistance in sample processing was provided by the University of North Carolina Center for Gastrointestinal Biology and Disease. Paraffin samples from indicated genetic backgrounds were stained in a uniform fashion using well-established methods within the clinical laboratory at the Brigham and Women's Hospital Pathology Immunohistochemical laboratory. Briefly, five micron sections were cut, and immunohistochemical staining for either Ki-67 (rabbit polyclonal, NCL-Ki67p, Novocastra), adrenocorticorticotropic hormone (ACTH; DAKO, N1531), prolactin (PRL; DAKO, N1549), growth hormone (GHR; DAKO, L1814), leutinizing hormone (LH; DAKO, L1827), follicle-stimulating hormone (FSH; DAKO, L1810), B220 (BD Biosciences/PharMingen, 557390), or CD3 (Serotec, MCA1477) was done using highly sensitive DAKO EnVision polymerized horseradish peroxidase detection methods. The proliferative index of the pituitary was calculated by counting only the cells in the intermediate pituitary: (total Ki67 + cells) / (total intermediate pituitary cells). The islet proliferative index was calculated on a per-islet basis as (total Ki67 + islet cells) / (total number of islet cells) per islet for each sample.

Taqman real-time PCR. Expression of mRNA was analyzed by quantitative Taqman real-time PCR as previously described, with some modifications (24). Reactions were carried out using cDNA equivalent to 80 ng RNA and done in triplicate for each sample. 18S rRNA was used as a loading control for all reactions. Primer sets for 18S (Hs99999901_s1), *p15*^{Ink4b} (Mm00483241_m1), *p18*^{Ink4c} (Mm00483243_m1), *p19*^{Ink4d} (Mm00486943_m1), *p21*^{Cip1} (Mm00432448_m1), and *p27*^{Kip1} (Mm00438167_g1) were purchased from Applied Biosystems; *p16*^{Ink4a} and *p19*^{Arf} primers were designed as previously described (25).

Statistics. Analysis of Kaplan-Meier survival curves was done using the log-rank test for each genotype pair. Proliferative index and islet size were not distributed normally and, therefore, were compared using a nonparametric (Mann-Whitney) test. High-density seeding was evaluated using the Student's unpaired t test. All error bars represent SE.

Results

***In vitro* growth and transformation of MEFs lacking *p16*^{Ink4a} and *p18*^{Ink4c}.** *Wild-type* MEFs show significant expression of $p16^{Ink4a}$ that markedly increases with serial passage (26, 27); yet, *p16*^{Ink4a}-deficient MEFs enter senescence with identical kinetics as *wild-type* cells (17, 18). MEFs lacking *p18*^{Ink4c} (16), *p19*^{Ink4d} (14), or both (28) also show no differences in life span despite significant expression of these proteins in cultured MEFs (27). In contrast, *p15*$^{Ink4b-/-}$ MEFs show a modest extension of life span (16), and cells carrying the Ink4-insensitive *cdk*^{R24C} mutation are immortal in culture (29, 30). Serial passage of *p16*$^{Ink4a-/-}$;*p18*$^{Ink4c-/-}$ MEFs revealed identical proliferation and life span as *wild-type* MEFs (Fig. 1*A*), and these cells entered senescence with identical kinetics as *wild-type* cells. Additionally, *p16*$^{Ink4a-/-}$;*p18*$^{Ink4c-/-}$ MEFs showed similar cdk and cyclin D1 expression (Fig. 1*B*) with serial passage.

In an effort to understand the underlying mechanisms driving MEF proliferation, we assessed the kinase activity of cdk4 and cdk2 with serial passage. As expected, cdk2 kinase activity decreased with passage, correlating highly with the onset of senescence (Fig. 1*C*). Surprisingly, cdk4 activity actually increased with passage, with its highest level of activity when cells were entering senescence (Fig. 1*C*). This increased cdk4 activity is likely due to the increased cyclin D protein and mRNA levels seen at late passage (Fig. 1*B*; data not shown). Although *p16*$^{Ink4a-/-}$;*p18*$^{Ink4c-/-}$ MEFs showed slightly increased cdk4 kinase activity compared with wild-type cells at all passages (Fig. 1*D*), there was little effect on proliferative life span (Fig. 1*A*). These data suggest that $p16^{Ink4a}$ and $p18^{Ink4c}$ regulate cdk4 kinase activity in MEFs, but these increases in cdk4 activity do not increase their proliferation, which seems to be predominantly determined by cdk2 kinase activity.

We additionally examined the effects of Ink4 deficiency on other aspects of MEF behavior *in vitro*. Growth arrest to high density in MEFs is partially mediated by $p16^{Ink4a}$ (22), but a role for $p18^{Ink4c}$ has not been explored. We assessed the ability of $p18^{Ink4c}$ to cooperate with *p16*^{Ink4a} loss in the regulation of high-density growth. Plates were re-fed but not passaged for 21 days and then assessed for cell number. Compared with *wild-type* cells, *p16*$^{Ink4a-/-}$;*p18*$^{Ink4c-/-}$ MEFs showed a 45% increase in cell number (P = 0.011; data not shown), comparable to the effect seen with loss of *p16*^{Ink4a} alone (22). As has been previously reported for *p16*$^{Ink4a-/-}$ (18, 22) and *p18*$^{Ink4c-/-}$ (16) MEFs, transformation by *H-ras*^{V12G} alone or *H-Ras*^{V12G} + *SV40 T-Ag* was not significantly different between *wild-type*, *p16*$^{Ink4a-/-}$, *p18*$^{Ink4c-/-}$, or *p16*$^{Ink4a-/-}$;*p18*$^{Ink4c-/-}$ MEFs (data not shown). These data confirm an effect of $p16^{Ink4a}$ on density arrest in MEFs but suggest only at most a modest role for $p16^{Ink4a}$ and $p18^{Ink4c}$ in resisting *Ras*-mediated transformation in MEFs.

***p16*$^{Ink4a-/-}$;*p18*$^{Ink4c-/-}$ mice develop aggressive pituitary tumors.** To analyze the effects of combined *p16*^{Ink4a} and *p18*^{Ink4c} deficiency *in vivo*, we generated mice lacking *p16*^{Ink4a} and/or *p18*^{Ink4c}. Both *p16*^{Ink4a} and *p18*^{Ink4c} lie on the murine chromosome 4, requiring a modified breeding scheme similar to that reported for mice lacking *p15*^{Ink4b} and *p18*^{Ink4c} (16). *p16*$^{Ink4a-/-}$;*p18*$^{Ink4c-/-}$ mice were produced in the expected ratio based on calculated frequency of recombination between *p16*^{Ink4a} and *p18*^{Ink4c}, were

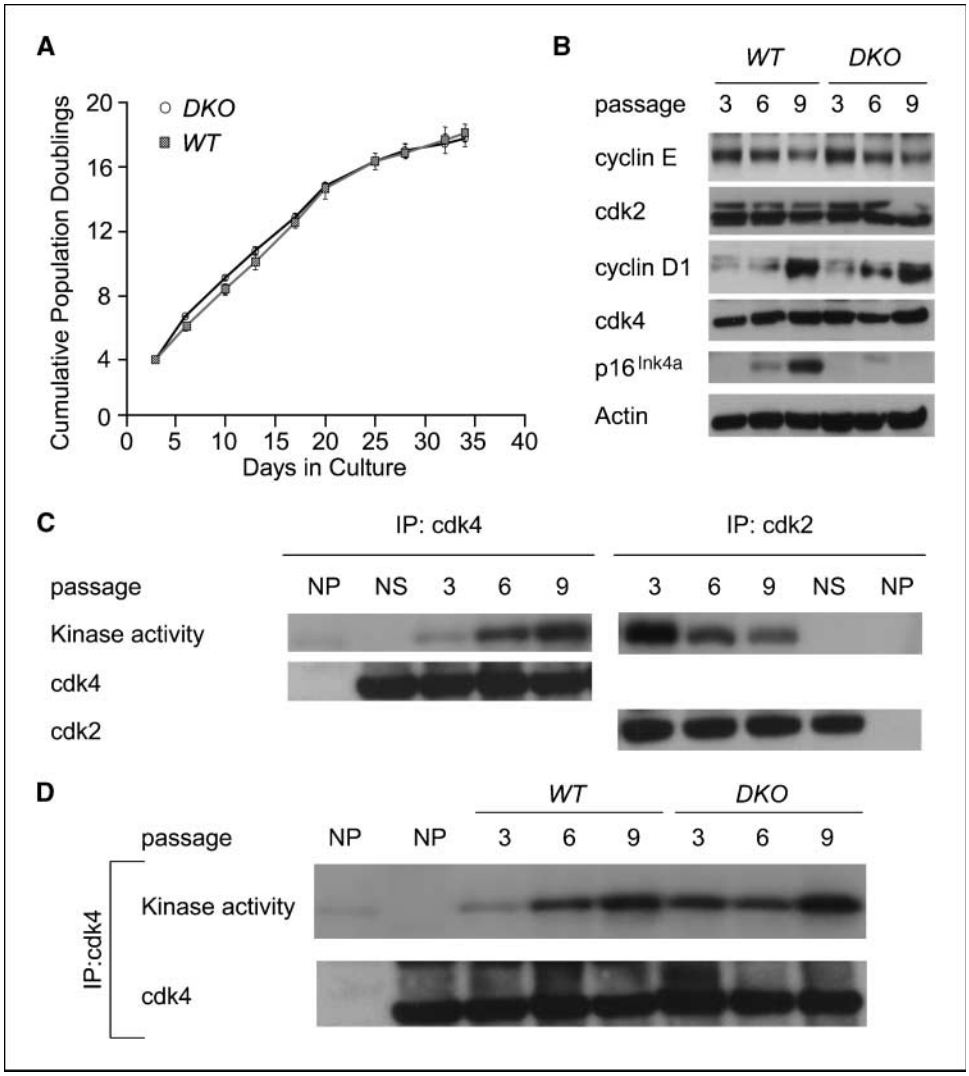

Figure 1. $p16^{Ink4a-/-};p18^{Ink4c-/-}$ MEFs show enhanced cdk4 kinase activity. *A,* life span of *wild-type* (*WT*) and $p16^{Ink4a-/-};p18^{Ink4c-/-}$ (*DKO*) MEFs grown according to standard 3T9 protocols at 21% O_2, 5% CO_2. Four to six lines were assessed per genotype. *Points,* mean; *bars,* SE. *B,* levels of cyclin E, cdk2, cyclin D1, cdk4, and $p16^{Ink4a}$ in asynchronously growing *wild-type* and $p16^{Ink4a-/-};p18^{Ink4c-/-}$ MEFs of indicated passage. Actin serves as a loading control. *C, in vitro* cdk4 (*left*) and cdk2 (*right*) kinase activity of *wild-type* MEFs with passage (*top*). Cdk4 or cdk2 complexes were immunoprecipitated (*IP*) from MEFs using either 900 μg (cdk4) or 100 μg (cdk2) total cell lysate. Kinase activity was assessed against GST-Rb-769 substrate. *NP,* no primary antibody. *NS,* no Rb substrate. One sixth of the total cdk4 or cdk2 immunoprecipitated is shown as loading control (*bottom*). *D, in vitro* cdk4 kinase activity of *wild-type* and $p16^{Ink4a-/-};p18^{Ink4c-/-}$ MEFs (*top*). Cdk4 complexes were immunoprecipitated from MEFs of indicated passage using 900 μg total cell lysate. Kinase activity was assessed against GST-Rb-769 substrate. One sixth of total cdk4 immunoprecipitated is shown as loading control (*bottom*).

fertile, and exhibited normal behavior. No significant difference in body weight was found between $p16^{Ink4a-/-};p18^{Ink4c-/-}$ and *wild-type* or $p16^{Ink4a+/-};p18^{Ink4c+/-}$ mice in this mixed genetic background. With aging, $p16^{Ink4a-/-};p18^{Ink4c-/-}$ mice showed increased morbidity with a median tumor-free survival of 42.7 weeks, compared with 68.8 weeks for $p18^{Ink4c-/-}$ mice ($P < 0.001$) and >70 weeks for $p16^{Ink4a-/-}$ mice ($P = 0.005$; Fig. 2*A*), showing strong cooperation between loss of $p16^{Ink4a}$ and $p18^{Ink4c}$ in promoting tumorigenesis.

Morbidity was associated with large pituitary tumors of the intermediate lobe, in some cases producing non-communicating hydrocephalus, hind limb paralysis, and/or pontine compression (Fig. 2*B*). Although pituitary tumors were found in all $p16^{Ink4a-/-};p18^{Ink4c-/-}$ mice examined over 30 weeks of age, $p18^{Ink4c-/-}$ mice developed pituitary tumors as previously reported (16, 20), with ~50% penetrance by 1 year. No pituitary tumors were found in $p16^{Ink4a-/-}$ mice at any age examined. $p16^{Ink4a-/-};p18^{Ink4c-/-}$ mice developed non-pituitary tumors (e.g., lymphomas and sarcomas) at a comparable frequency to that of $p16^{Ink4a-/-}$ mice (data not shown), suggesting that cooperation between $p16^{Ink4a}$ and $p18^{Ink4c}$ in tumor suppression was most marked in the pituitary. Although this observation is in accord with previous findings showing an important anticancer role of cdk4/6 regulation in tumorigenesis of the intermediate pituitary (20, 30), loss of $p18^{Ink4c}$ combined with loss of $p15^{Ink4b}$ (16) or $p19^{Ink4d}$ (28) did not appreciably accelerate pituitary formation nor increase incidence, suggesting that $p16^{Ink4a}$ plays a predominant role in the prevention of pituitary tumorigenesis in $p18^{Ink4c-/-}$ mice.

In an effort to understand the basis of this cooperation, we did gross, histologic, and molecular analysis of age-matched *wild-type,* $p16^{Ink4a-/-}$, $p18^{Ink4c-/-}$, and $p16^{Ink4a-/-};p18^{Ink4c-/-}$ mice. Inspection of pituitaries of 35-week-old mice revealed normal macroscopic and microscopic structure in *wild-type* and $p16^{Ink4a-/-}$ mice (Fig. 2*C*). Consistent with previous data (20), $p18^{Ink4c-/-}$ mice at this age showed hyperplasia of the intermediate lobe with modest associated disruption of the gland architecture. However, $p16^{Ink4a-/-};p18^{Ink4c-/-}$ mice showed a marked increase in the size of the pituitary and anatomic disarray of the intermediate lobe with near complete effacement of the posterior lobe (Fig. 2*C*). Similar to $cdk4^{R24C}$ knock-in mice (30), cystic degeneration, hemorrhage, and necrosis were commonly seen in the pituitaries of $p16^{Ink4a-/-};p18^{Ink4c-/-}$ mice, even in animals less than 20 weeks of age, but were rarely seen in $p18^{Ink4c-/-}$ mice. Pituitary tumors in $p16^{Ink4a-/-};p18^{Ink4c-/-}$ mice stained strongly for ACTH, but not for

other peptide hormones (PRL, GH, LH, or FSH) made in the pituitary (Fig. 2*D*), suggesting tumors were of the adrenocorticotroph lineage. Additionally, blood serum levels of α-MSH increased with age in $p16^{Ink4a-/-};p18^{Ink4c-/-}$ mice (Supplementary Fig. S1), as was reported for $Rb^{+/-}$ mice (31). These data suggest that $p16^{Ink4a}$ serves to limit tumor progression in the intermediate pituitary of $p18^{Ink4c-/-}$ mice.

$p16^{Ink4a}$ functionally compensates for $p18^{Ink4c}$ loss in the pituitary. To determine the functional consequences of combined $p16^{Ink4a}$ and $p18^{Ink4c}$ loss, we determined the Ki67 proliferative index in the intermediate lobe of the pituitary in adult mice. The intermediate lobes of the pituitary in 35-week-old *wild-type*, $p16^{Ink4a-/-}$, $p18^{Ink4c-/-}$, and $p16^{Ink4a-/-};p18^{Ink4c-/-}$ mice were compared. The rate of proliferation was comparable in *wild-type* (0.4%) and $p16^{Ink4a-/-}$ (0.5%) mice but significantly increased in $p18^{Ink4c-/-}$ mice (1.9%, $P < 0.05$ for both pairwise comparisons). Mice lacking both $p16^{Ink4a}$ and $p18^{Ink4c}$ showed an even greater increase in proliferation (2.7%) above *wild-type* ($P = 0.003$), $p16^{Ink4a-/-}$ ($P < 0.001$), and $p18^{Ink4c-/-}$ mice ($P = 0.09$; Fig. 3*A*). This result suggests that the increase in $p16^{Ink4a}$ expression partially compensates for $p18^{Ink4c}$ loss in the intermediate pituitary, even in animals of intermediate (35-week-old) age.

To understand the mechanistic basis for this cooperation in tumors, we did an analysis of cdk inhibitor expression in the pituitary of *wild-type* and $p18^{Ink4c-/-}$ mice. Although there was a modest increase in *Arf* (3.4-fold), $p21^{Cip1}$ (2.3-fold), $p15^{Ink4b}$ (2.4-fold), and $p19^{Ink4d}$ (1.5-fold) mRNA in $p18^{Ink4c-/-}$ mice when compared with *wild-type* mice, expression of $p16^{Ink4a}$ mRNA was by far the most increased (18.2-fold) in the pituitary of young (10.6-week-old) $p18^{Ink4c-/-}$ mice (Fig. 3*B*). Consistent with previous findings (20), $p18^{Ink4c-/-}$ mice of this age exhibited only mild hyperplasia with no evidence of tumors and had overtly normal

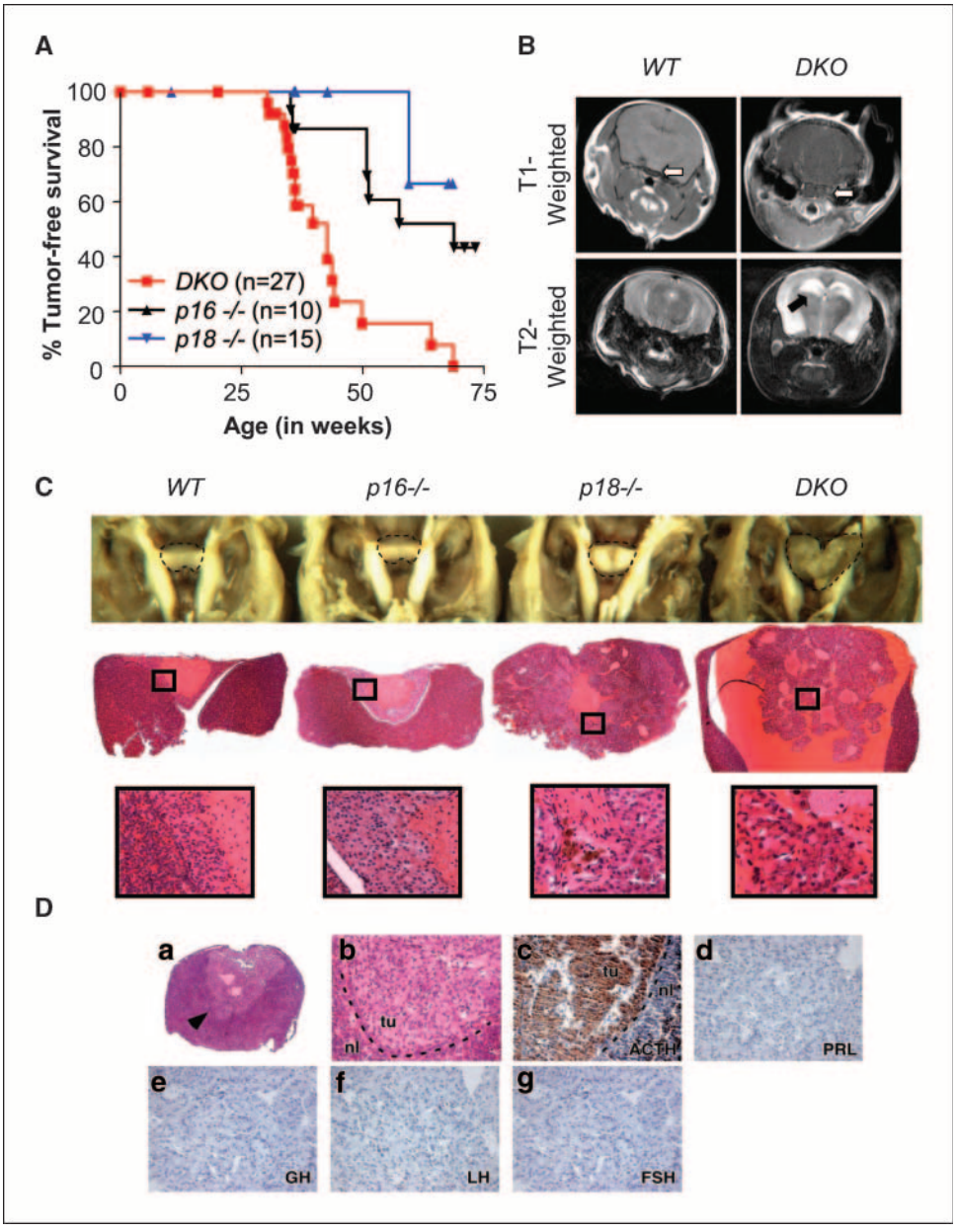

Figure 2. Mice lacking $p16^{Ink4a}$ and $p18^{Ink4c}$ develop pituitary tumors. *A,* tumor-free survival of mice lacking $p16^{Ink4a}$ and/or $p18^{Ink4c}$. The control groups consisted of $p16^{Ink4a+/+};p18^{Ink4c-/-}$ ($n = 14$) or $p16^{Ink4a-/-};p18^{Ink4c+/+}$ ($n = 10$) and were compared with the $p16^{Ink4a-/-};p18^{Ink4c-/-}$ ($n = 27$) group. Mean survival: $p16^{Ink4a-/-};p18^{Ink4c-/-}$ mice, 42.7 wks; $p18^{Ink4c-/-}$ mice, 68.8 wks; $p16^{Ink4a-/-}$ mice, >70 wks. *B,* magnetic resonance images of *wild-type* (*left*) and $p16^{Ink4a-/-};p18^{Ink4c-/-}$ (*right*) mice at 44 wks of age. T1-weighted images (*top*) are at the level of the pituitary (*white arrow*). T2-weighted images (*bottom*) are taken at the level of the ventricles. Note marked hydrocephalus (*black arrow*) in the mouse on right. Compare with normal image of *wild-type* mouse (*left*). *C,* representative gross samples and H&E staining of pituitaries of indicated genotypes at 35 wks of age. Pituitary in gross samples is outlined (*dashed line*). *D,* immunohistochemistry of hyperplastic intermediate lobe from $p16^{Ink4a-/-};p18^{Ink4c-/-}$ mouse at 35 wks of age. Note the tumor stains for ACTH but not PRL, GH, LH, or FSH, indicating that tumor cells are adrenocorticotroph in origin. ACTH and α-MSH are cleavage products derived from the same precursor molecule proopiomelanocortin.

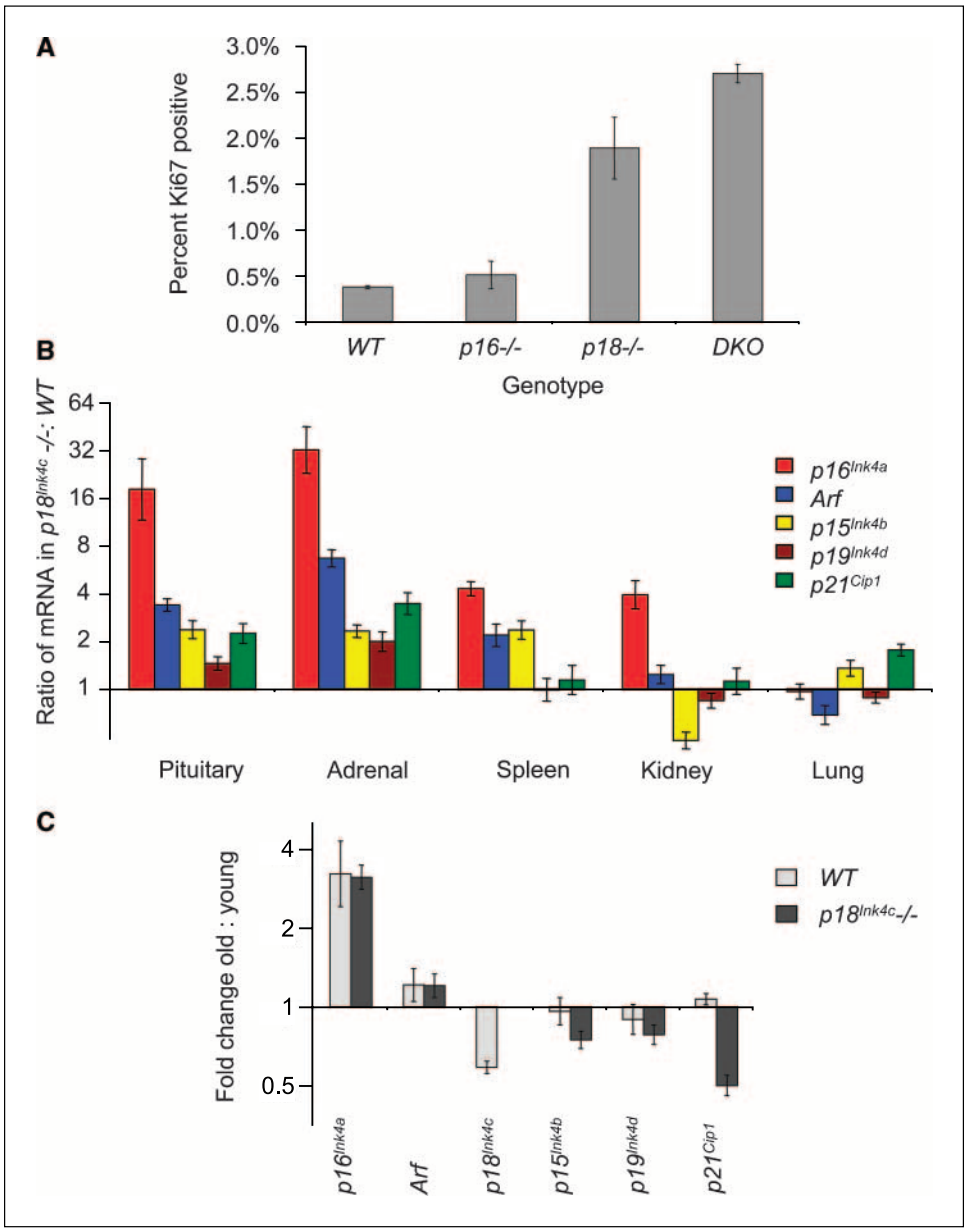

Figure 3. $p18^{Ink4c-/-}$ mice have increased $p16^{Ink4a}$ mRNA levels in specific tissues. *A,* quantification of proliferative index in the pituitary of 35-wk-old *wild-type*, $p16^{Ink4a-/-}$, $p18^{Ink4c-/-}$, and $p16^{Ink4a-/-}$;$p18^{Ink4c-/-}$ mice. At least two mice per genotype were used, and all cells in the intermediate lobe were counted for each pituitary. *Columns,* mean; *bars,* SE. *B,* relative mRNA expression by real-time PCR of $p16^{Ink4a}$, *Arf*, $p15^{Ink4b}$, $p19^{Ink4d}$, and $p21^{Cip1}$ in indicated tissue of 10.6-wk-old *wild-type* and $p18^{Ink4c-/-}$ mice. Ratio of expression of indicated gene in $p18^{Ink4c-/-}$ mice compared with *wild-type* littermates. At least two to six mice per genotype were assayed; samples were measured in triplicate. 18S RNA served as a loading control and normalization. *Columns,* mean; *bars,* SE. *C,* relative increase in mRNA expression of $p16^{Ink4a}$, *Arf*, $p18^{Ink4c}$, $p15^{Ink4b}$, $p19^{Ink4d}$, and $p21^{Cip1}$ in the pituitary with aging. Ratio of fold increase in old (54–59 wks) versus young (10.6 wks) is shown by $p18^{Ink4c}$ genotype. At least two mice per genotype were assayed; samples were measured in duplicate. *Columns,* mean; *bars,* SE.

tissue architecture (data not shown). Although this analysis does not exclude an effect of $p18^{Ink4c}$ deficiency on the protein expression of other cell cycle regulators, such as $p27^{Kip1}$ (20), it suggests a potent *in vivo* mechanism of compensation for germline $p18^{Ink4c}$ deficiency by increased transcription of $p16^{Ink4a}$.

Previous studies have shown that $p16^{Ink4a}$ expression increases with age in most mammalian tissues (24, 25, 27), and we noted that total pituitary similarly exhibited an increase in $p16^{Ink4a}$ expression with aging (Fig. 3*C*). A comparable age-induced induction of $p16^{Ink4a}$ expression was noted in $p18^{Ink4c-/-}$ mice such that the ratio of $p16^{Ink4a}$ expression in old (~57-week-old) versus young (10.6-week-old) pituitary was the same for *wild-type* or $p18^{Ink4c-/-}$ mice (Fig. 3*C*). Therefore, old $p18^{Ink4c-/-}$ mice showed a >40-fold increase in the mRNA expression of $p16^{Ink4a}$ compared with young *wild-type* mice, indicating the additive induction of $p16^{Ink4a}$ in this compartment in response to aging and $p18^{Ink4c}$ deficiency.

$p16^{Ink4a}$ and $p18^{Ink4c}$ coordinately control proliferation in the islets. To determine if the effect of combined Ink4 loss was seen in other tissues, we considered the pancreatic islet from 35-week-old mice (29, 32–34). As previously reported for $p18^{Ink4c-/-}$ mice (34), we found that $p16^{Ink4a-/-}$;$p18^{Ink4c-/-}$ mice showed a modest increase in median islet size compared with *wild-type* and $p16^{Ink4a-/-}$ mice (Supplementary Fig. S2). There was no discernable difference in islet size between $p18^{Ink4c-/-}$ and $p16^{Ink4a-/-}$;$p18^{Ink4c-/-}$ mice in animals of this age. Double staining with Ki67 and insulin indicated that the majority (>80%) of proliferating islet cells were β-cells (data not shown), whose replication is regulated by cdk4, $p18^{Ink4c}$, and cyclin D2 in the adult (32–35). In mice of this age, no significant difference in proliferation was seen between *wild-type* (0.58%), $p16^{Ink4a-/-}$ (0.67%), or $p18^{Ink4c-/-}$ (0.71%) islets for any pairwise comparison (Supplementary Fig. S2). However, $p16^{Ink4a-/-}$;$p18^{Ink4c-/-}$ islets

had a significantly higher rate of proliferation (0.98%) than *wild-type* ($P = 0.02$), *p16Ink4a−/−* ($P = 0.08$), and *p18Ink4c−/−* ($P = 0.02$) islets. It is important to note that these studies were carried out in young mice, and we expect that the effects of *p16Ink4a* loss would be more pronounced in older mice, as *p16Ink4a* expression potently inhibits islet proliferation in an age-dependent manner (24, 25). In aggregate, these data suggest that p16Ink4a and p18Ink4c coordinately regulate cdk4/6-dependent proliferation in the pancreatic β-cells of adult mice.

Ink4 family members can transcriptionally compensate for loss of other members. To determine if the increase in *p16Ink4a* mRNA in the pituitary was tissue specific, we examined other tissues from *p18Ink4c−/−* mice. *p16Ink4a* levels were elevated in the adrenal glands (32.3-fold), spleen (4.3-fold), and kidney (3.9-fold) of *p18Ink4c−/−* mice, but there was no discernable change in *p16Ink4a* in the lung (Fig. 3*B*). The pituitary, adrenal glands, and spleen also showed moderately elevated levels of *Arf* and *p15Ink4b*, but little change was seen in the kidney or the lung. These results suggest that loss of *p18Ink4c* induces expression of other cdk inhibitors, specifically *p16Ink4a* in a tissue specific fashion *in vivo*.

It is possible that changes in cdk inhibitor levels could be a non–cell-autonomous effect due increased *in vivo* proliferation from *p18Ink4c* loss. We thus turned our attention to a more purified cell system (MEFs), which express all four Ink4 proteins (27). An examination of wild-type MEFs showed a massive increase in expression in all three transcripts from the *Ink4/Arf* locus (*p15Ink4b*, *p16Ink4a*, and *Arf*) in the first few days of culture, which was not seen for *p18Ink4c* and *p19Ink4d* (Fig. 4*A*). However, only *p16Ink4a* continued to increase throughout passage, whereas mRNA levels of *Arf*, *p15Ink4b*, *p18Ink4c*, *p19Ink4d*, *p21Cip1*, and *p27Kip1* remained relatively constant.

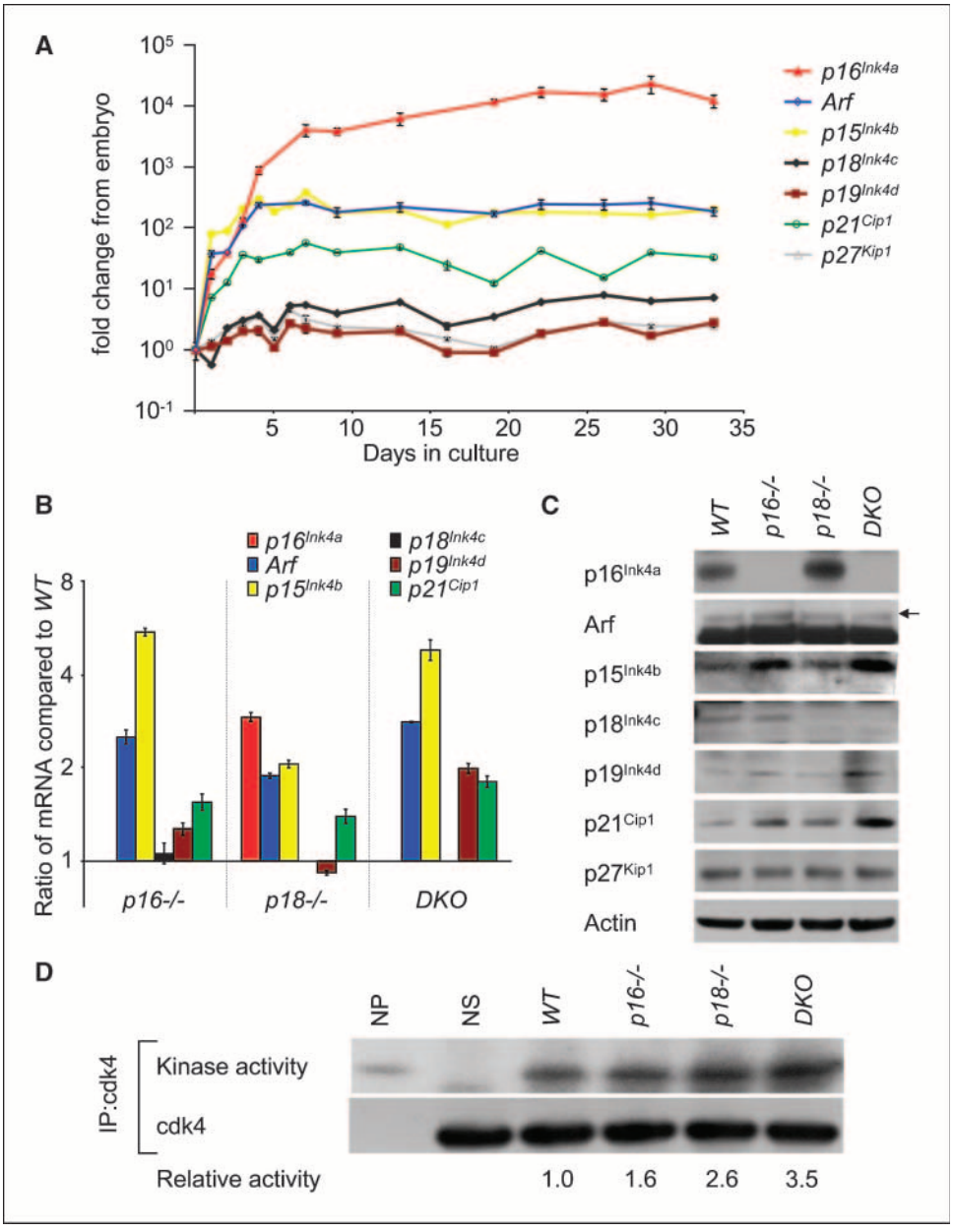

Figure 4. MEFs show transcriptional compensation between Ink4 proteins. *A,* relative mRNA expression of *p16Ink4a*, *Arf*, *p15Ink4b*, *p18Ink4c*, *p19Ink4d*, *p21Cip1*, and *p27Kip1* in cultured *wild-type* MEFs. Fold change from E13.5 embryo, which has not been put in culture. At least two lines per genotype were assayed; samples were measured in triplicate. 18S RNA served as a loading control and normalization. *Points,* mean; *bars,* SE. *B,* real-time PCR of *p16Ink4a*, *Arf*, *p15Ink4b*, *p18Ink4c*, *p19Ink4d*, and *p21Cip1* in MEFs. Mid–life span (~10 population doublings) MEFs lacking *p16Ink4a* or *p18Ink4c* or both (*DKO*) were assessed for mRNA levels of indicated cdk inhibitors. Fold change from *wild-type* levels. 18S RNA served as a loading control and normalization. *Columns,* mean; *bars,* SE. *C,* Western blot analysis of p16Ink4a, Arf, p15Ink4b, p18Ink4c, p19Ink4d, p21Cip1, and p27Kip1. Mid–life span (~10 population doublings) *wild-type*, *p16Ink4a−/−*, *p18Ink4c−/−*, and *p16Ink4a−/−;p18Ink4c−/−* MEFs were analyzed for protein expression. Actin serves as a loading control. *Arrow,* specific band in Arf blot. *D, in vitro* cdk4 kinase activity of *wild-type*, *p16Ink4a−/−*, *p18Ink4c−/−*, and *p16Ink4a−/−;p18Ink4c−/−* MEFs (*top*). Cdk4 complexes were immunoprecipitated from mid–life span (~10 population doublings) MEFs using 900 μg total cell lysate. Kinase activity was assessed against GST-Rb-769 substrate. One sixth of the total cdk4 immunoprecipitated is shown as loading control (*bottom*). Relative activity represents fold difference from *wild type*.

We then examined mid–life span MEFs (~10 population doublings) for cdk inhibitor expression. $p16^{Ink4a-/-}$ MEFs had a significant increase in $p15^{Ink4b}$ (5.5-fold), moderate increases in Arf (2.5-fold) and $p21^{Cip1}$ (1.6-fold) and a slight increase in $p19^{Ink4d}$ (1.3-fold) at both the mRNA (Fig. 4*B*) and protein (Fig. 4*C*) levels when compared with *wild-type* MEFs. As was seen in the various tissues *in vivo* (Fig. 3*B*), $p18^{Ink4c-/-}$ MEFs showed the greatest increase in $p16^{Ink4a}$ levels (2.9-fold) and more modest change in Arf (1.9-fold), $p21^{Cip1}$ (1.4-fold), and $p15^{Ink4b}$ (2.1-fold), with little change in $p19^{Ink4d}$ (0.9-fold). MEFs lacking both $p16^{Ink4a}$ and $p18^{Ink4c}$ showed a large difference in the expression of $p15^{Ink4b}$ (4.8-fold) and smaller increases for Arf (2.8-fold), $p21^{Cip1}$ (1.8-fold), and $p19^{Ink4d}$ (2.0-fold). There were no detectable differences in $p27^{Kip1}$ mRNA (data not shown) or protein (Fig. 4*C*) between genotypes. Interestingly, all changes in mRNA levels were closely mirrored by changes in protein expression, suggesting that protein and message correlate highly under these conditions (compare Fig. 4*B* and *C*). Importantly, the compensation among the ink4 proteins is not complete, as $p16^{Ink4a-/-}$, $p18^{Ink4c-/-}$, and $p16^{Ink4a-/-};p18^{Ink4c-/-}$ MEFs show elevated cdk4 kinase activity (Fig. 4*D*) compared with *wild-type* cells. In aggregate, these results suggest that increased cdk4 activity due to loss of Ink4 proteins can be partially compensated for through activation of either $p15^{Ink4b}$ or $p16^{Ink4a}$ both *in vitro* and *in vivo*.

Cdk4/6 kinase activity is required for proliferation in specific compartments in adult mice. Genetic data have suggested a role for cdk4 in the regulation of proliferation in the pituitary and the pancreatic islets (20, 29, 33–35). We have found that these tissues show increased proliferation in mice lacking the cdk4/6 inhibitors $p16^{Ink4a}$ and $p18^{Ink4c}$ (Fig. 3*A*; Supplementary Fig. S2), suggesting a role for cdk4/6 catalytic activity in the regulation of these tissues in adult mice. However, cdk4/6 kinase activity is required for development of certain embryonic tissues, leading to late embryonic lethality in cyclin D (36) or cdk4/6 (37) null animals, thus limiting the ability to examine adult tissues. To address this issue, we determined the effect of acute cdk4/6 inhibition in 26-week-old $p16^{Ink4a-/-};p18^{Ink4c-/-}$ mice using PD 0332991, a specific inhibitor of cdk4/6, but not cdk2 or other tested kinases (38). PD 0332991 is a pyrido(2,3-*d*)pyrimidin-7-one compound modified with a 2-aminopyridine side chain that has been shown to block the growth of pRB-competent human cell lines and xenografted tumors with potent activity at nanomolar concentrations. PD 0332991 shows good oral bioavailability and can be given to mice for prolonged treatment with minimal toxicity (21, 38). Comparable to its potency in human cells, PD 0332991 was shown to inhibit murine cdk4 activity at doses as low as 50 nmol/L, whereas cdk2 activity was not affected even at micromolar concentrations (Fig. 5*A*).

To investigate the effects of cdk4/6 inhibition in adults, animals were treated with 150 mg/kg PD 0332991 by oral gavage daily for 2 weeks. As previously reported (21), this dose and schedule were well tolerated by the mice without evident toxicity. In accord with the phenotype observed in the $p16^{Ink4a-/-};p18^{Ink4c-/-}$ mice, both the pituitary and pancreatic islets showed a marked reduction in proliferation after treatment with PD 0332991 (Fig. 5*B* and *C*). Consistent with the reported hyperproliferation in germinal center B cells in $p18^{Ink4c}$-deficient animals (39), we found that the majority of proliferating cells in $p16^{Ink4a-/-};p18^{Ink4c-/-}$ lymph nodes express the B-cell marker B220 and not CD3, a T-cell marker (data not shown). As was seen in the islet and pituitary, treatment with PD 0332991 inhibited proliferation of these hyperproliferative B cells in the germinal centers of lymph node (Fig. 5*B*). These data suggest that the pancreatic islet, intermediate pituitary, and germinal center B lymphocytes require the catalytic activity of cdk4/6 for proliferation in adult mice.

Unlike the islet and pituitary, however, proliferation in other tissues was not affected by prolonged cdk4/6 inhibition. The high rate of proliferation seen in the small bowel was not changed after 2 weeks of PD 0332991 treatment (Fig. 5*B* and *C*). In addition, a subset of B220-negative and CD3-negative cells dispersed throughout the lymph nodes continued to proliferate despite cdk4/6 inhibition (Fig. 5*D*). The morphology, location, and frequency of these cells seem most consistent with inter-digitating dendritic cells of the lymph node. Although it is formally possible that PD 0332991 is excluded from certain proliferating compartments, a more likely explanation is that proliferation of some cell types in adult mice do not require cdk4/6 activity.

Discussion

$p16^{Ink4a}$ and $p18^{Ink4c}$ cooperate to suppress tumorigenesis in mice. The elucidation of the redundant contributions of individual genes in a highly related family is a problem in the study of mammalian biology, particularly in the case of the Ink4 family of cdk inhibitors. All four proteins are capable of binding cdk4 and cdk6 (2–5), and there seems to be little biochemical distinction among the Ink4s with regard to this activity (12). Therefore, it is not surprising that there is significant compensation by remaining Ink4s in MEFs singly deficient for $p16^{Ink4a}$ and $p18^{Ink4c}$. However, *Ink4*-null mice show marked phenotypic differences, indicating distinct roles for these proteins *in vivo*. An examination of $p15^{Ink4b-/-};p18^{Ink4c-/-}$ (16) and $p19^{Ink4d-/-};p18^{Ink4c-/-}$ (28) mice has led to elucidation of some of the unique functions of Ink4 proteins, and we have expanded on this data through generation of mice lacking both $p16^{Ink4a}$ and $p18^{Ink4c}$.

Our data suggest that $p16^{Ink4a}$ and $p18^{Ink4c}$ are important determinants of physiologic and neoplastic proliferation in certain tissues *in vivo*. For example, $p18^{Ink4c}$ seemed to regulate homeostatic islet and pituitary proliferation in young mice, and this effect was constrained by $p16^{Ink4a}$ expression (Fig. 3, Fig. 4*A*, and Fig. 5*B*; Supplementary Fig. S2). Loss of both proteins potently cooperated in pituitary tumorigenesis in our study; whereas the tumor spectrum, frequency, and latency in $p18^{Ink4c-/-}$ mice was not augmented by additional loss of $p15^{Ink4b}$ (16) or $p19^{Ink4d}$ (28). Although high penetrance of lethal pituitary tumors limited the finding of new tumor types, the latency of lethal pituitary tumors in $p16^{Ink4a-/-};p18^{Ink4c-/-}$ mice was much shorter than either single knockout, with survival comparable to mice with $cdk4^{R24C}$ mutation, which does not bind Ink4 proteins (29, 30). Analysis of Ink4 levels in several tissues suggested an explanation for the cooperation seen between $p16^{Ink4a}$ and $p18^{Ink4c}$ loss: only $p16^{Ink4a}$ expression was significantly increased in the pituitary of $p18^{Ink4c-/-}$ mice, and not $p15^{Ink4b}$ or $p19^{Ink4d}$. This compensation is not limited to the pituitary, where there was an obvious phenotype, but was also seen in other tissues to varying degrees and in cultured MEFs (Fig. 3*B* and Fig. 4*B* and *C*). These results suggest a potent feedback mechanism for regulating cdk4/6 in the response to increased kinase activity.

Control of $p16^{Ink4a}$ expression by Rb-family protein function has been noted in several systems where inactivation of Rb leads to a

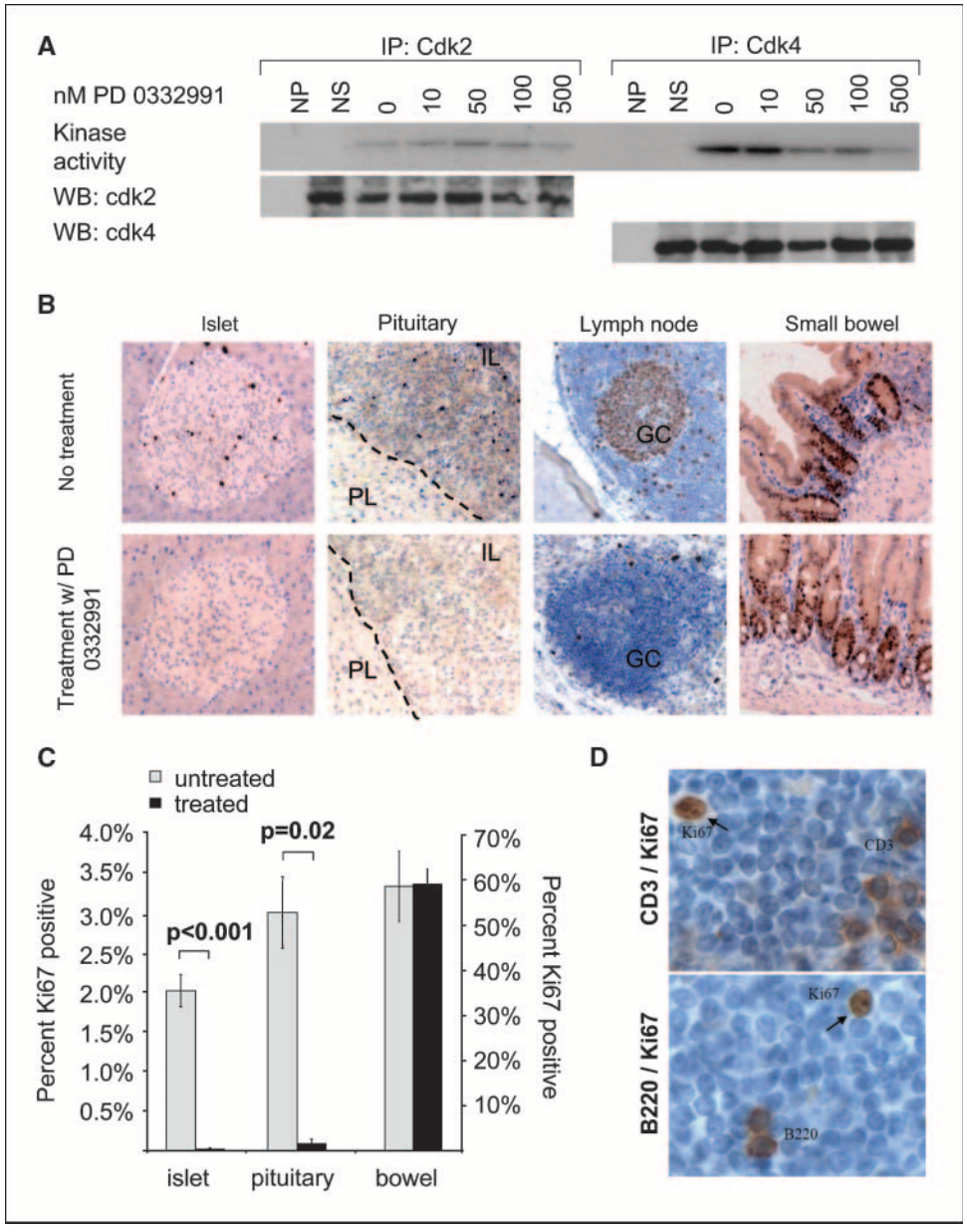

Figure 5. Inhibition of cdk4/6 blocks proliferation in some but not all tissues. *A,* PD 0332991 effectively inhibits murine cdk4 but not cdk2 kinase activity in $p16^{Ink4a-/-};p18^{Ink4c-/-}$ MEFs. *In vitro* cdk2 and cdk4 kinase assay of $p16^{Ink4a-/-};p18^{Ink4c-/-}$ MEFs after 24 h of treatment with varying concentrations of PD 0332991. Cdk2 or cdk4 complexes were immunoprecipitated, and kinase activity was assessed against GST-Rb-769 substrate. Note that more protein (900 versus 100 μg) was used for cdk4 immunoprecipitation than for cdk2 immunoprecipitation. *B,* inhibition of cdk4/6 blocks proliferation in some tissues. Ki67 staining of pancreatic islets, pituitary, lymph nodes, and small bowel of 26-wk-old $p16^{Ink4a-/-};p18^{Ink4c-/-}$ mice. Mice were treated with vehicle (*top*) or 150 mg/kg PD 0332991 (*bottom*) for 2 wks. *PL,* posterior lobe; *IL,* intermediate lobe; *GC,* germinal center. *C,* quantification of proliferation in the pancreatic islets, intermediate pituitary, and small bowel of 26-wk-old $p16^{Ink4a-/-};p18^{Ink4c-/-}$ mice with and without 2 wks treatment with 150 mg/kg PD 0332991. Cells were counted from at least two mice per genotype, with at least 400 cells counted for the small bowel. Proliferation in pancreatic β-cells was determined as average proliferation per islet from at least 38 islets of at least two mice per genotype. Pituitary proliferation was assessed as proliferative index of the entire intermediate lobe of at least two mice. *Columns,* mean; *bars,* SE. Magnification, ×20 (all photos). *D,* lymph nodes from 26-wk-old $p16^{Ink4a-/-};p18^{Ink4c-/-}$ mice treated for 2 wks with 150 mg/kg PD 0332991 were stained for Ki67 and CD3 or B220. Note that Ki67 positive cells (nuclear) do not stain for either CD3 or B220 (cell surface markers). Therefore, Ki67-positive cells in PD 0332991–treated mice are neither T cells nor B cells.

rapid increase in $p16^{Ink4a}$ expression (40, 41). Likewise, $p16^{Ink4a}$ can be activated by overexpression of E2F (42), arguing for the presence of a feedback loop between Rb and $p16^{Ink4a}$. Clearly, however, physiologic proliferation with attendant Rb family phosphorylation is not generally sufficient to activate $p16^{Ink4a}$ expression. Instead, Rb loss only seems to activate $p16^{Ink4a}$ expression under specific circumstances (e.g., neoplastic growth). Recent work has suggested a possible explanation for the conditional regulation of $p16^{Ink4a}$ by Rb. Kotake et al. (43) have shown that the Polycomb group (PcG) protein Bmi-1, which durably represses of $p16^{Ink4a}$ expression in association with covalent histone modifications (44, 45), is targeted to the *Ink4a/Arf* locus by Rb family proteins. Additionally, Bmi-1 seems to require Rb family function to stably repress $p16^{Ink4a}$ expression in human and murine cells. Therefore, it is tempting to speculate that $p16^{Ink4a}$ expression (and possibly that of $p15^{Ink4b}$ and *Arf* as well) is increased in certain $p18^{Ink4c}$-deficient tissues because of a relative hyperphosphorylation of pRb with attendant decrease in the PcG-mediated repression of the *Ink4a/Arf* locus.

Certain adult tissues require cdk4/6 activity. Recent genetic experiments have suggested that MEFs can proliferate without cdk4 (32, 33), cdk6 (37), or both (36, 37). Conversely, cdk2 kinase activity is also dispensable in MEFs, as $cdk2^{-/-}$ (46, 47) and $cyclin\ E1^{-/-};cyclin\ E2^{-/-}$ (48) cells can proliferate in culture, albeit more slowly. Although cdk4/6 activity was not a major determinant of MEF proliferation, this was not true in certain tissues *in vivo* such as the intermediate pituitary, germinal center B cells, and pancreatic β-cell. In these tissues, the specific requirement of cdk4/6 catalytic activity was supported by our findings that genetic loss of $p16^{Ink4a}$ and $p18^{Ink4c}$ resulted in their increased proliferation, whereas acute pharmacologic inhibition abrogated their proliferation.

The dependence of pancreatic β-cells cells on cdk4 for proliferation seems restricted to postnatal mice, as $cdk4^{-/-}$ mice

are born with islets, but cannot sustain proliferation as the animal grows (32, 33). Conversely, loss of cdk4 regulation by *p18^{Ink4c}* loss (34), *p16^{Ink4a}* loss (25), or knock-in of *cdk4^{R24C}* (29, 30, 33) results in aberrant proliferation in the pancreatic β-cells. In aggregate, these results indicate an exclusive role for cdk4 in the regulation of pancreatic β-cell proliferation in the adult mouse. Additionally, some tissues are regulated both prenatally and postnatally by cdk4/6. We have shown that B cells require cdk4/6 for proliferation in the adult animal, but they are also required in the developing embryo, as both D-deficient and cdk4/6-deficient mice die with greatly reduced common lymphoid progenitors (36, 37). Most importantly, *cdk4/6$^{-/-}$* and *cyclin-D1/D2/D3$^{-/-}$* mice show that the absolute requirement for cdk4/6 in development seems to hold in only a few select tissue compartments, as substantial development occurs in their absence (36, 37). Our data using a specific cdk4/6 inhibitor further these developmental observations to show that adult mice similarly only require cdk4/6 in a limited number of compartments, including B cells, pituitary adrenocortotrophs, and pancreatic β-cells; compartments where *p16$^{Ink4a-/-}$;p18$^{Ink4c-/-}$* mice show the most marked phenotype.

In summary, we have shown that p16^{Ink4a} compensates for *p18^{Ink4c}* loss to regulate neoplastic and physiologic proliferation. Additionally, by both pharmacologic and genetic approaches, we have shown that p16^{Ink4a} and p18^{Ink4c} function *in vivo* to constrain cdk4/6 catalytic activity in highly specific compartments. The search for effective Cdk inhibitors has been hampered by lack of clarity over the best Cdk to target and the challenge of achieving appropriate levels of kinase selectivity. Our data show that cdk4/6 kinase activity is directly responsible for regulating proliferation of specific tissue compartments in adult mice and thus help to predict the toxicity of specific cdk4/6 inhibitors. Additionally, these data offer hope that certain established cancers (e.g., those characterized by *cdk4* mutation, *cyclin D* amplification, or *p16^{Ink4a}* loss) will also strictly require cdk4/6 activity for proliferation and therefore respond to specific pharmacologic inhibition of these kinases.

Acknowledgments

Received 9/18/2006; revised 2/1/2007; accepted 3/12/2007.

Grant support: Sidney Kimmel Foundation for Cancer Research, NIH grants AG 024379 and DK34987, and NIH Cell and Molecular Biology Training program grant GM008581 (M.R. Ramsey).

The costs of publication of this article were defrayed in part by the payment of page charges. This article must therefore be hereby marked *advertisement* in accordance with 18 U.S.C. Section 1734 solely to indicate this fact.

We thank Peter Toogood, Diego Castrillon, Lishan Su, Grigory Kovalev, Paula Miliani de Marval, Feng Bai, Stuart Shumway, Chad McCall, and Kathy Wilber for advice, reagents, and technical assistance and Robert Duronio and William Kim for critical reading of the manuscript.

References

1. Malumbres M, Barbacid M. Mammalian cyclin-dependent kinases. Trends Biochem Sci 2005;30:630–41.
2. Serrano M, Hannon GJ, Beach D. A new regulatory motif in cell-cycle control causing specific inhibition of cyclin D/CDK4. Nature 1993;366:704–7.
3. Hannon GJ, Beach D. p15INK4B is a potential effector of TGF-beta-induced cell cycle arrest. Nature 1994;371:257–61.
4. Guan KL, Jenkins CW, Li Y, et al. Growth suppression by p18, a p16INK4/MTS1- and p14INK4B/MTS2-related CDK6 inhibitor, correlates with wild-type pRb function. Genes Dev 1994;8:2939–52.
5. Hirai H, Roussel MF, Kato JY, Ashmun RA, Sherr CJ. Novel INK4 proteins, p19 and p18, are specific inhibitors of the cyclin D-dependent kinases CDK4 and CDK6. Mol Cell Biol 1995;15:2672–81.
6. Ruas M, Peters G. The p16INK4a/CDKN2A tumor suppressor and its relatives. Biochim Biophys Acta 1998;1378:F115–77.
7. Brotherton DH, Dhanaraj V, Wick S, et al. Crystal structure of the complex of the cyclin D-dependent kinase Cdk6 bound to the cell-cycle inhibitor p19INK4d. Nature 1998;395:244–50.
8. Russo AA, Tong L, Lee JO, Jeffrey PD, Pavletich NP. Structural basis for inhibition of the cyclin-dependent kinase Cdk6 by the tumour suppressor p16INK4a. Nature 1998;395:237–43.
9. Thullberg M, Bartek J, Lukas J. Ubiquitin/proteasome-mediated degradation of p19INK4d determines its periodic expression during the cell cycle. Oncogene 2000;19:2870–6.
10. Phelps DE, Hsiao KM, Li Y, et al. Coupled transcriptional and translational control of cyclin-dependent kinase inhibitor p18INK4c expression during myogenesis. Mol Cell Biol 1998;18:2334–43.
11. Gump J, Stokoe D, McCormick F. Phosphorylation of p16INK4A correlates with Cdk4 association. J Biol Chem 2003;278:6619–22.
12. Thullberg M, Bartkova J, Khan S, et al. Distinct versus redundant properties among members of the INK4 family of cyclin-dependent kinase inhibitors. FEBS Lett 2000;470:161–6.
13. Sharpless NE. INK4a/ARF: a multifunctional tumor suppressor locus. Mutat Res 2005;576:22–38.
14. Zindy F, van Deursen J, Grosveld G, Sherr CJ, Roussel MF. INK4d-deficient mice are fertile despite testicular atrophy. Mol Cell Biol 2000;20:372–8.
15. Chen P, Zindy F, Abdala C, et al. Progressive hearing loss in mice lacking the cyclin-dependent kinase inhibitor Ink4d. Nat Cell Biol 2003;5:422–6.
16. Latres E, Malumbres M, Sotillo R, et al. Limited overlapping roles of P15(INK4b) and P18(INK4c) cell cycle inhibitors in proliferation and tumorigenesis. EMBO J 2000;19:3496–506.
17. Krimpenfort P, Quon KC, Mooi WJ, Loonstra A, Berns A. Loss of p16Ink4a confers susceptibility to metastatic melanoma in mice. Nature 2001;413:83–6.
18. Sharpless NE, Bardeesy N, Lee KH, et al. Loss of p16Ink4a with retention of p19Arf predisposes mice to tumorigenesis. Nature 2001;413:86–91.
19. Sharpless NE, Ramsey MR, Balasubramanian P, Castrillon DH, DePinho RA. The differential impact of p16(INK4a) or p19(ARF) deficiency on cell growth and tumorigenesis. Oncogene 2004;23:379–85.
20. Franklin DS, Godfrey VL, Lee H, et al. CDK inhibitors p18(INK4c) and p27(Kip1) mediate two separate pathways to collaboratively suppress pituitary tumorigenesis. Genes Dev 1998;12:2899–911.
21. Fry DW, Harvey PJ, Keller PR, et al. Specific inhibition of cyclin-dependent kinase 4/6 by PD 0332991 and associated antitumor activity in human tumor xenografts. Mol Cancer Ther 2004;3:1427–38.
22. Sharpless NE, Alson S, Chan S, Silver DP, Castrillon DH, DePinho RA. p16(INK4a) and p53 deficiency cooperate in tumorigenesis. Cancer Res 2002;62:2761–5.
23. Miliani de Marval PL, Macias E, Rounbehler R, et al. Lack of cyclin-dependent kinase 4 inhibits c-*myc* tumorigenic activities in epithelial tissues. Mol Cell Biol 2004;24:7538–47.
24. Krishnamurthy J, Torrice C, Ramsey MR, et al. Ink4a/Arf expression is a biomarker of aging. J Clin Invest 2004;114:1299–307.
25. Krishnamurthy J, Ramsey MR, Ligon KL, et al. p16INK4a induces an age-dependent decline in islet regenerative potential. Nature 2006;443:453–7.
26. Palmero I, McConnell B, Parry D, et al. Accumulation of p16INK4a in mouse fibroblasts as a function of replicative senescence and not of retinoblastoma gene status. Oncogene 1997;15:495–503.
27. Zindy F, Quelle DE, Roussel MF, Sherr CJ. Expression of the p16INK4a tumor suppressor versus other INK4 family members during mouse development and aging. Oncogene 1997;15:203–11.
28. Zindy F, den Besten W, Chen B, et al. Control of spermatogenesis in mice by the cyclin D-dependent kinase inhibitors p18(Ink4c) and p19(Ink4d). Mol Cell Biol 2001;21:3244–55.
29. Sotillo R, Dubus P, Martin J, et al. Wide spectrum of tumors in knock-in mice carrying a Cdk4 protein insensitive to INK4 inhibitors. EMBO J 2001;20:6637–47.
30. Rane SG, Cosenza SC, Mettus RV, Reddy EP. Germ line transmission of the Cdk4(R24C) mutation facilitates tumorigenesis and escape from cellular senescence. Mol Cell Biol 2002;22:644–56.
31. Hu N, Gutsmann A, Herbert DC, Bradley A, Lee WH, Lee EY. Heterozygous Rb-1 delta 20/+ mice are predisposed to tumors of the pituitary gland with a nearly complete penetrance. Oncogene 1994;9:1021–7.
32. Tsutsui T, Hesabi B, Moons DS, et al. Targeted disruption of CDK4 delays cell cycle entry with enhanced p27(Kip1) activity. Mol Cell Biol 1999;19:7011–9.
33. Rane SG, Dubus P, Mettus RV, et al. Loss of Cdk4 expression causes insulin-deficient diabetes and Cdk4 activation results in beta-islet cell hyperplasia. Nat Genet 1999;22:44–52.
34. Pei XH, Bai F, Tsutsui T, Kiyokawa H, Xiong Y. Genetic evidence for functional dependency of p18Ink4c on Cdk4. Mol Cell Biol 2004;24:6653–64.
35. Georgia S, Bhushan A. Beta cell replication is the primary mechanism for maintaining postnatal beta cell mass. J Clin Invest 2004;114:963–8.
36. Kozar K, Ciemerych MA, Rebel VI, et al. Mouse development and cell proliferation in the absence of D-cyclins. Cell 2004;118:477–91.
37. Malumbres M, Sotillo R, Santamaria D, et al. Mammalian cells cycle without the D-type cyclin-dependent kinases Cdk4 and Cdk6. Cell 2004;118:493–504.
38. Toogood PL, Harvey PJ, Repine JT, et al. Discovery of a potent and selective inhibitor of cyclin-dependent kinase 4/6. J Med Chem 2005;48:2388–406.
39. Tourigny MR, Ursini-Siegel J, Lee H, et al. CDK inhibitor p18(INK4c) is required for the generation of functional plasma cells. Immunity 2002;17:179–89.
40. Tam SW, Shay JW, Pagano M. Differential expression and cell cycle regulation of the cyclin-dependent kinase 4 inhibitor p16Ink4. Cancer Res 1994;54:5816–20.

41. Li Y, Nichols MA, Shay JW, Xiong Y. Transcriptional repression of the D-type cyclin-dependent kinase inhibitor p16 by the retinoblastoma susceptibility gene product pRb. Cancer Res 1994;54:6078–82.
42. Khleif SN, DeGregori J, Yee CL, et al. Inhibition of cyclin D-CDK4/CDK6 activity is associated with an E2F-mediated induction of cyclin kinase inhibitor activity. Proc Natl Acad Sci U S A 1996;93:4350–4.
43. Kotake Y, Cao R, Viatour P, Sage J, Zhang Y, Xiong Y. pRB family proteins are required for H3K27 trimethylation and Polycomb repression complexes binding to and silencing p16INK4alpha tumor suppressor gene. Genes Dev 2007;21:49–54.
44. Jacobs JJ, Kieboom K, Marino S, DePinho RA, van Lohuizen M. The oncogene and Polycomb-group gene bmi-1 regulates cell proliferation and senescence through the ink4a locus. Nature 1999; 397:164–8.
45. Itahana K, Zou Y, Itahana Y, et al. Control of the replicative life span of human fibroblasts by p16 and the polycomb protein Bmi-1. Mol Cell Biol 2003;23: 389–401.
46. Berthet C, Aleem E, Coppola V, Tessarollo L, Kaldis P. Cdk2 knockout mice are viable. Curr Biol 2003;13: 1775–85.
47. Ortega S, Prieto I, Odajima J, et al. Cyclin-dependent kinase 2 is essential for meiosis but not for mitotic cell division in mice. Nat Genet 2003;35:25–31.
48. Geng Y, Yu Q, Sicinska E, et al. Cyclin E ablation in the mouse. Cell 2003;114:431–43.

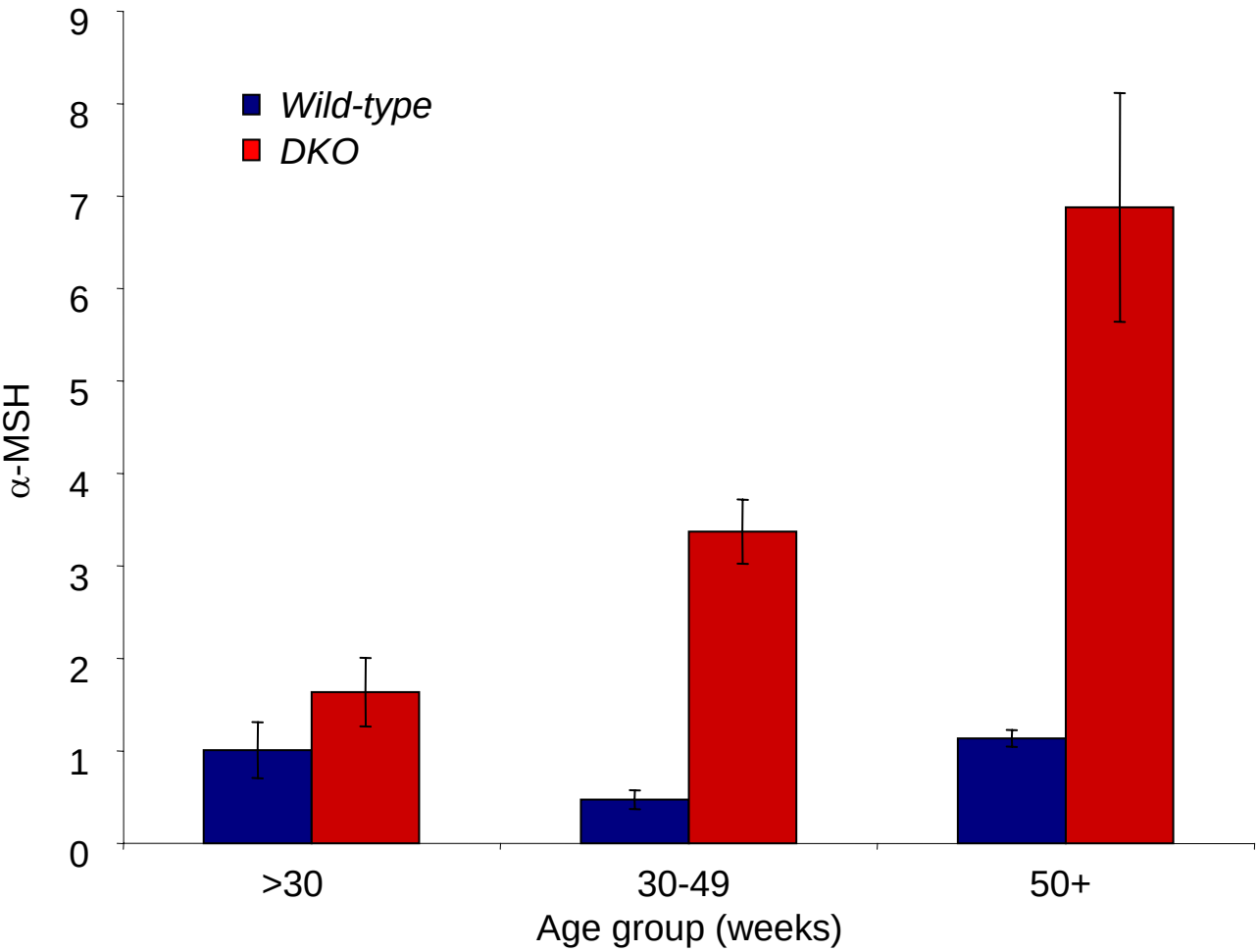

Ramsey et al, Supplemental Figure 1

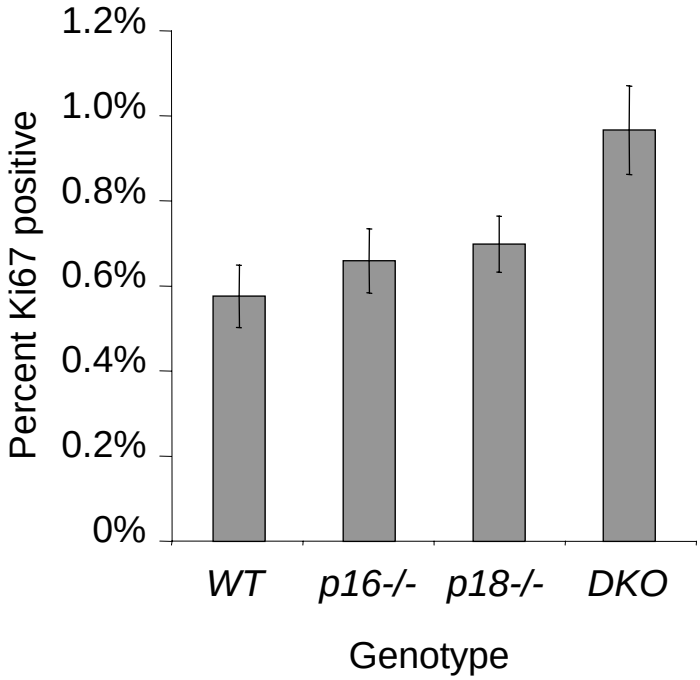

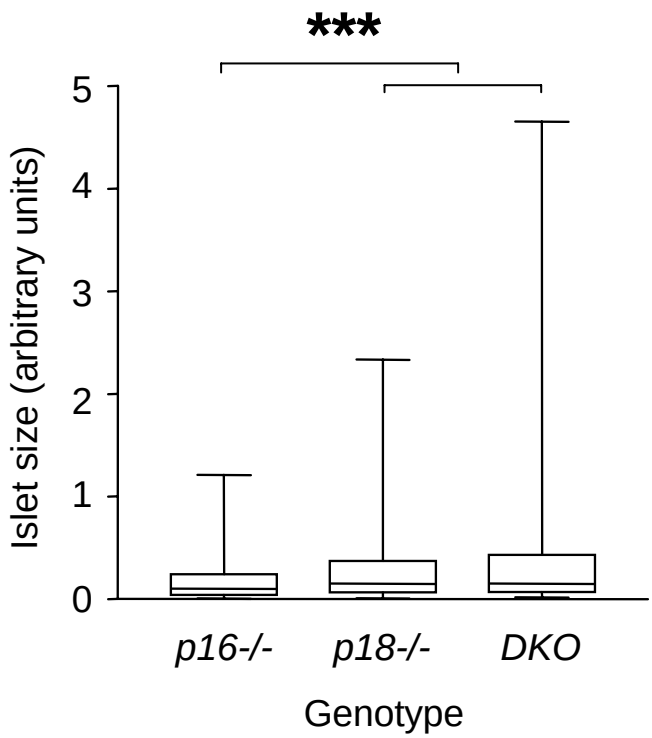

Ramsey et al, Supplemental Figure 2

Supplemental Figure Legends

Supplemental Figure 1

Average values of α-MSH in *wild-type* and *p16^{Ink4a}-/-; p18^{Ink4c}-/-* mice with increasing age. At least 4 mice per genotype were assayed for each group. Error bars indicate +/- SEM.

Supplemental Figure 2

(a) Quantification of proliferative index in the pancreatic islets of 35 week old *wild-type* (*WT*), *p16^{Ink4a}-/-*, *p18^{Ink4c}-/-*, and *p16^{Ink4a}-/-; p18^{Ink4c}-/-* (*DKO*) mice. At least 2 mice per genotype and at least 42 islets per genotype were counted. Error bars indicate +/- SEM.

(b) Islet size of *p16^{Ink4a}-/-*, *p18^{Ink4c}-/-*, and *p16^{Ink4a}-/-; p18^{Ink4c}-/-* (*DKO*) mice at 35 weeks. Between 115 and 215 islets were counted from at least two mice per genotype. Boxes represent median size and 25-75% data range, while whiskers represent entire range of data, ***$p<0.001$.